PIBB 生物化学与生物物理进展
Progress in Biochemistry and Biophysics
2014, 41(8): 787~795
www.pibb.ac.cn

Whole Genome RNAi Screen in *C. elegans* Identifies CAB-1 as a Novel Regulator of DCV Secretion*

XIA Zhi-Ping[1,3)**], CHEN Yan[1,3)**], SHENG Yi[1,2)], YI Ya-Lan[1,3)], SONG E-Li[1)***], XU Tao[1,2)***]
([1)] *National Laboratory of Biomacromolecules, Institute of Biophysics, Chinese Academy of Sciences, Beijing* 100101, China;
[2)] *College of Life Science and Technology, Huazhong University of Science and Technology, Wuhan* 430074, China;
[3)] *University of Chinese Academy of Sciences, Beijing* 100049, China)

Abstract The dense core vesicle (DCV) is a key organelle involved in the secretion of hormones and neuropeptides in endocrine cells and neurons in response to stimulation. However, the mechanisms underlying its biogenesis, trafficking and exocytosis remain largely unknown. In this study, to discover novel players functioning in DCV secretion, we performed a genome-wide RNAi screen in *C. elegans* by observing worm defecation behavior. A series of genes that function in the intestine to regulate DCV biogenesis or exocytosis were successfully identified, including CAB-1, which was further determined to be a specific regulator for DCV exocytosis. In the intestine, *cab-1* mutation causes reduced secretion of intestinal DCV cargoes. In the nervous system, the loss of CAB-1 leads to the accumulation of DCV markers in the presynaptic region, but synaptic vesicles are not affected. This work demonstrates that CAB-1 is a regulatory factor specifically involved in DCV secretion.

Key words CAB-1, defecation, dense core vesicle (DCV), secretion, whole genome RNAi screen
DOI: 10.3724/SP.J.1206.2014.00047

Neurons communicate with other cells through the secretion of different signaling molecules such as neurotransmitters and neuropeptides, which are stored in synaptic vesicles (SVs) and dense core vesicles (DCVs), respectively [1–2]. Compared with SVs, much less is known about DCVs, especially the mechanisms underlying its biogenesis, trafficking and exocytosis. Generally, DCVs are formed at the *trans*-Golgi network (TGN) as immature DCVs (iDCVs). After budding from the TGN, iDCVs undergo several maturation steps, including homotypic fusion of iDCVs, which is mediated by SNARE proteins [3–5], gradual acidification by the action of vacuolar ATPases [6–8] and clathrin-dependent removal of non-DCV cargoes [9–10]. During the maturation process, prohormones and proneuropeptides undergo proteolytic cleavage by prohormone convertases, resulting in the formation of mature molecules that are then crystallized in the form of the dense cores in DCVs. Mature DCVs (mDCVs) are then transported to the distal release site along microtubules and released on demand[11–12].

Both DCVs and SVs are membrane-enclosed organelles for neurotransmission, and they share numerous components in their exocytosis process, including the SNARE complex and the calcium sensor synaptotagmin [1, 13]. However, molecular regulators specifically for DCVs have not been extensively characterized. Among the limited discoveries, UNC-31 and PKC-1, two conserved proteins identified in *C. elegans*, are well-defined participants [14–16]. Thus,

*This work was supported by grants from National Basic Research Program of China (2010CB833701), The National Natural Science Foundation of China (31130065, 31270884, 31300701) and The Beijing Natural Science Foundation (5122026).
**These authors contributed equally to this work.
***Corresponding author. Tel: 86-10-64888469
XU Tao. E-mail: xutao@ibp.ac.cn
SONG E-Li. E-mail: songali@moon.ibp.ac.cn
Received: February 21, 2014 Accepted: April 16, 2014

efforts need be made to identify novel components to elucidate the mechanisms involved in the exocytosis of DCVs.

Large-scale RNAi screen is a powerful method that has been widely used to systematically identify new regulators of various biological processes, and it is especially successfully used in *C. elegans*, because RNAi can easily be introduced into worms by injection[17], by soaking the worms directly in dsRNA[18] or by feeding the worms with bacteria strains that express specific dsRNAs[19]. Since two independent but overlapping RNAi bacteria libraries, which together cover 94% of the *C. elegans* genes, were created[20-21], whole genome RNAi screen have become a common strategy in *C. elegans*. For example, Lynch *et al*[22]. identified MAGI-1 as an L1CAM-dependent stabilizer of apical junctions from a genome-wide functional RNAi screen, and Morton *et al*[23]. found new contributors to early embryonic polarity in a par mutant enhancer screen. However, a systematic screen for genes involved in DCV exocytosis has not been reported.

In *C. elegans*, the expulsion (Exp) step of the defecation motor program (DMP) has been demonstrated to be regulated by signaling molecules secreted from the intestine[24]. For example, NLP-40, which is synthesized in the intestine and stored in DCVs, has been recently identified as a signaling molecule[25] that triggers the Exp step of DMP. Therefore, mutation of regulatory factors involved in intestinal DCV secretion is thought to cause defects in *C. elegans* defecation behavior. Based on this principle, to discover novel players functioning in DCV exocytosis, we performed a whole genome RNAi screen by observing DMP in *C. elegans*. Multiple genes that function in the intestine were successfully identified, and several of these genes were reported to be involved in the biogenesis or secretion of DCVs. Additionally, we provided evidences that CAB-1 affected intestinal DCV secretion, and we further demonstrated that CAB-1 also functioned in the nervous system to regulate the exocytosis of DCVs, but not SVs. To the best of our knowledge, this research is the first to report that CAB-1 is a novel regulator specific for DCV exocytosis.

1 Materials and methods

1.1 *C. elegans* strains

The following strains were used in this study: N2, *cab-1* (*tg46*), *rbf-1* (*js232*), *oxIs206* [*Paex-3*::*proANF*::*gfp*], *ceIs72*[*Punc-129*::*ida-1*::*gfp*], *nuIs152*[*Punc-129*::*snb-1*::*gfp*], *jsIs1072* [*Pvha-6*::*aex-5*::*venus*] and *Is* [*Pnlp-40*::*nlp-40*::*yfp*]. All the strains were maintained using standard methods[26].

1.2 Whole genome RNAi screen

The RNAi screen procedures were performed as previously described (Figure 1a and ref [27]). Briefly, the RNAi bacterial strains were incubated at 37℃ for ~16 h and then were seeded onto individual RNAi plates. After ~24 h, approximately 50 of the synchronized L1 worms were added to each plate. After 3 days of RNAi treatment at 20℃, the adult worms were scored under a dissecting microscope for the DMP defect. Only the pBoc and Exp steps were observed. The empty vector L4440 and *aex-5* strain were used as controls. Genes were considered to be PCs when more than three out of ten defective DMPs were observed. All the PCs were scored for a second round of RNAi treatment to confirm the phenotype.

1.3 Phenotype analysis

For the DMP phenotypes, individual adult worm was picked to NGM plate seeded with OP50, and after 5 min, ten consecutive DMPs were observed under the dissecting microscope. Only the pBoc and Exp steps were scored, and the aBoc step was omitted. The cycle length was calculated as the time between two pBocs. For developmental phenotypes, synchronized L1 worms were placed on NGM plates seeded with OP50, and the worms that reached the young adult stage after 72 h were scored. The young adult worms were imaged using a ZEISS Discovery V8 microscope equipped with CCD, and the body size was analyzed using ImageJ software (National Institutes of Health). For brood size analysis, healthy early L4 worms were picked to individual plates seeded with OP50 and were transferred at the indicated time points to new plates. The live progeny were scored 24 h after transferring.

1.4 Integration

The OJ1160 *vjEx555*[*Pttx-3*::*rfp*, *Pnlp-40*::*nlp-40*::*yfp* at 1 mg/L] strain was used for integration using γ radiation according to standard methods[28]. Briefly, the L4 worms carrying the transgene were irradiated with γ radiation on an empty NGM plate. The worms were then recovered on the OP50 bacterial lawn for 4 h and were picked to new NGM plates individually as P0. In total, ~20 F2 from each P0 for strains with 100% transgene expression were scored. The integrated strains were backcrossed to N2 for at least 3 times

before being used for subsequent experiments.

1.5 Imaging

All confocal microscope images were acquired using an Olympus FV500 laser-scanning confocal microscope with a 60×[NA (numerical aperture)=1.40] oil objective. The confocal settings used for image capture were held constant in comparison experiments. The images were quantified and analyzed using ImageJ software (National Institutes of Health). Worm fluorescence imaging and quantification were performed according to methods previously described [15]. The max-pixel intensity in WT worms was set to an arbitrary fluorescence unit of 1.0 to enable comparisons with other strains.

1.6 Data analysis

Averaged results were presented as the means ± SEM. Statistical significance was evaluated using Student's *t* test. Asterisks denote statistical significance compared with the control, with *P* values less than 0.05 (*), 0.01 (**) and 0.001 (***).

2 Results

2.1 Whole genome RNAi screen identifies genes that affect DMP

The DMP is a highly regulated rhythmic behavior that initiates within the *C. elegans* intestine, which is recognized as the pacemaker of this behavior [25]. Signaling molecules secreted from the intestine trigger the downstream DVB and AVL neurons to execute the Exp step of DMP [24-25]. However, the mechanisms governing signaling molecule secretion in the intestine have not been completely clarified. We propose that knocking down genes that affect intestinal secretion would cause defects in Exp; therefore, we performed a whole genome RNAi screen using the *rbf-1* (*js232*) mutant (Figure 1a), which is slightly uncoordinated [29] and thus convenient for DMP observations.

The *rbf-1* (*js232*) mutant has normal DMPs but exhibits severe defects when treated with *aex-5* RNAi, which encodes a pro-protein convertase and functions in the intestine to regulate DMPs [24, 30] (Figure 1b), suggesting that intestinal DMP can be used as a reliable readout for the screen. The Ahringer and Vidal RNAi libraries were used for the screen. After the first round of screening, we identified 118 genes as potential candidates (PCs) when more than three defective DMPs were observed out of ten random DMPs (Table S1 in **Supplementary material**). All the PCs were selected for a second round of screen, and ten genes were confirmed to cause defects of greater than 50% in DMP (Figure 1c) when they were knocked-down. Among these genes, neuropeptide NLP-40 was recently reported as the essential signaling molecule secreted by the intestine, and its release was regulated by the calcium sensor synaptotagmin SNT-2 [25]. In addition, *hid-1* and *unc-108* mediated the maturation of DCVs [31-34], and *aex-1* and *aex-4* were participants in DCV exocytosis [24, 35]. *aex-5* and *egl-21*, two pro-protein processing enzymes that are co-packaged in DCVs [24, 36], were also identified. These results suggested that our screen is successful. However, *cab-1*, a novel gene previously

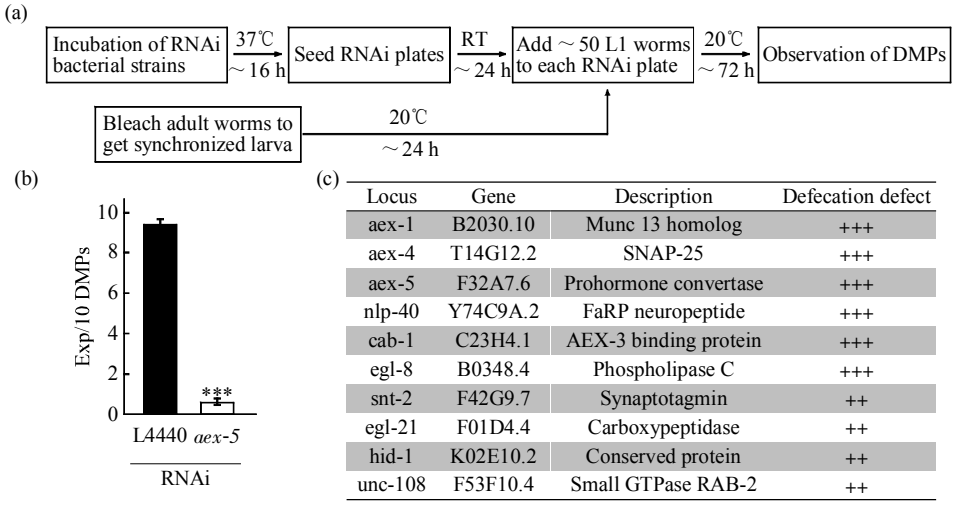

Locus	Gene	Description	Defecation defect
aex-1	B2030.10	Munc 13 homolog	+++
aex-4	T14G12.2	SNAP-25	+++
aex-5	F32A7.6	Prohormone convertase	+++
nlp-40	Y74C9A.2	FaRP neuropeptide	+++
cab-1	C23H4.1	AEX-3 binding protein	+++
egl-8	B0348.4	Phospholipase C	+++
snt-2	F42G9.7	Synaptotagmin	++
egl-21	F01D4.4	Carboxypeptidase	++
hid-1	K02E10.2	Conserved protein	++
unc-108	F53F10.4	Small GTPase RAB-2	++

Fig. 1　Whole genome RNAi screen identified genes that regulate the DMP in *C. elegans*

(a) Schematic illustrating the screening procedures. (b) *aex-5* was used as positive control: when treated with *aex-5* RNAi, the worms lost almost all the Exp steps. For both L4440 control and *aex-5* RNAi, at least 7 random observations were achieved. (c) Positive genes were listed. +++: greater than 80% of the DMPs were defective; ++: 50%~ 80% of the DMPs were defective.

identified as an AEX-3-binding protein in a yeast-two-hybrid screen[37], has not been reported to be associated with DCVs; therefore, we focused on this gene to explore its functions.

2.2 Phenotypic analyses of *cab-1*(*tg46*) mutants

The phenotypes of worms treated with *cab-1* RNAi looked quite similar to the worms treated with *aex-5* RNAi: both worms were constipated, small in body size, pale in color and slow growing (our observations and ref [30]). To further characterize the phenotypes caused by *cab-1* mutation, we obtained the *cab-1* (*tg46*) mutant from the CGC. As previously reported, *cab-1*(*tg46*) mutant lost greater than 90% of the Exp step in its DMPs (Figure 2a); however, the posterior body wall muscle contraction (pBoc) was not affected (data not shown). Meanwhile, the cycle length of the *cab-1*(*tg46*) worms was distributed over a more expanded range, and the average cycle length was slightly extended(Figure 2b). Additionally, *cab-1*(*tg46*) exhibited other phenotypes associated with development. For example, almost none of the *cab-1* (*tg46*) L1 larva reached the young adult stage after approximately 72 h, whereas most of the wild type (WT) worms reached this stage (Figure 2c). And the adult *cab-1* (*tg46*) mutant worms were smaller in body size than WT worms(Figure 2d). The *cab-1*(*tg46*) mutants also exhibited defects in brood size: WT worms stopped laying eggs ~96 h after early L4, and the total progeny number reached more than 200; in contrast, *cab-1*(*tg46*) worms produced only 60 progeny in 96 h (Figure 2e).

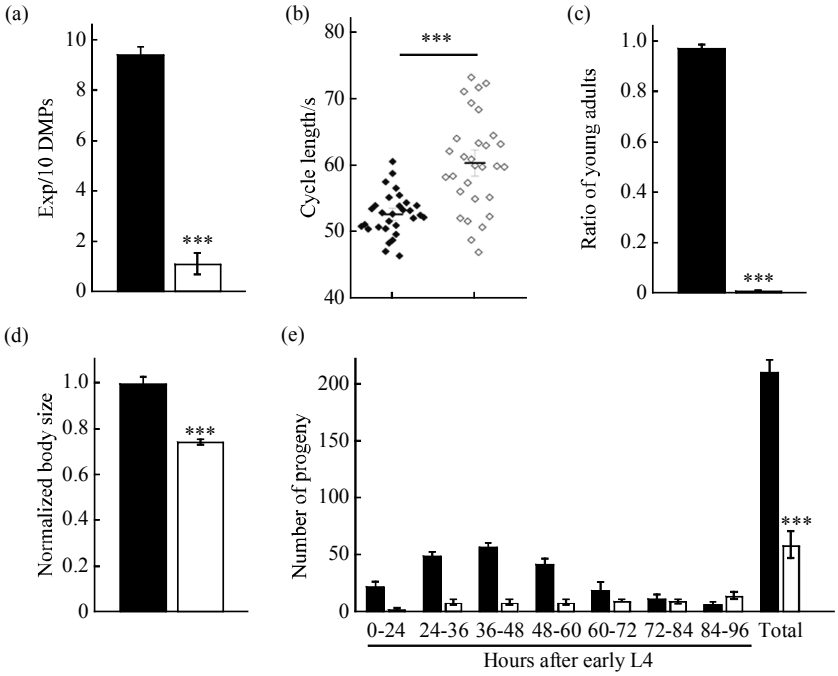

Fig. 2 *cab-1*(*tg46*) mutants showed both DMP and developmental defects

(a) *cab-1*(*tg46*) worms lost approximately 90% of Exps in the DMPs. n=7 for both WT and *cab-1*(*tg46*) mutants. (b) The cycle length of *cab-1*(*tg46*) had a more expanded range, and the average cycle length was longer. 30 cycles for both WT and *cab-1*(*tg46*) mutants. (c) *cab-1*(*tg46*) developed more slowly than WT: when the WT worms reached the young adult stage, almost none of the *cab-1*(*tg46*) worms had also reached this stage. n=6 for WT and *cab-1*(*tg46*) mutants. (d) Compared with the WT, the young adult *cab-1*(*tg46*) worms were smaller in body size. n=17 for WT and n=16 for *cab-1*(*tg46*) mutants. (e) *cab-1*(*tg46*) produced fewer progeny than the WT worms. n=9 for both WT and *cab-1*(*tg46*) mutants. ■: WT; □: *cab-1*(*tg46*).

2.3 CAB-1 modulates the secretion of DCV cargoes from the intestine

NLP-40 was recently reported as a key element to regulate DMPs in *C. elegans*[25]. NLP-40 is packaged in DCVs and is secreted from the intestine, and *nlp-40* mutant worms lost almost all of the Exp steps in the DMP cycle (Figure 1c and ref [25]), as was observed in the *cab-1* (*tg46*) mutants (Figure 2 and ref [37]). Therefore, we wondered whether the defecation defect observed in *cab-1* mutants was caused by the

insufficient secretion of NLP-40 from the intestine. First, we integrated the OJ1160 *vjEx555* [*Pttx-3*::*rfp*, *Pnlp-40*::*nlp-40*::*yfp* at 1 mg/L] strain to obtain a stable strain *Is* [*Pnlp-40*::*nlp-40*::*yfp*] (see **Materials and methods** for details). In this strain, NLP-40-YFP was distributed diffusely in the intestine, and the accumulated YFP signal was observed near the basolateral membrane, which may represent the DCVs that are ready for release (Figure 3). Using this strain, we examined the secretion of NLP-40-YFP in the *cab-1*(*tg46*) mutants by detecting the YFP fluorescence intensity in coelomocytes, which would take up the proteins secreted from other tissues into the body cavity. We observed that the YFP fluorescence intensity was dramatically decreased in the coelomocytes of the *cab-1* (*tg46*) mutants to approximately 30% of WT (Figure 3a). Notably, we found that the basolateral accumulation of NLP-40-YFP almost disappeared in the *cab-1* (*tg46*) mutants (Figure 3b), suggesting that the ready-to-release DCVs are reduced.

To further confirm this result, we employed another DCV marker, AEX-5-Venus, to detect intestinal secretion using *cab-1* RNAi, which could effectively knocked down CAB-1 in the intestine because the *C. elegans* intestine is very sensitive to RNAi treatment[38]. AEX-5 is a pro-protein convertase that functions in the intestine to regulate DMPs and is co-packaged into DCVs with other cargoes[24], enabling it to be used as a marker to detect intestinal secretion. Consistently, the AEX-5-Venus signal in the *cab-1* (*tg46*) coelomocytes was also sharply decreased to ~30% of the WT level (Figure 3c), similar to NLP-40-YFP. These results indicated that CAB-1 regulates intestinal DCV secretion, most likely by modulating the abundance of DCVs near the basolateral membrane.

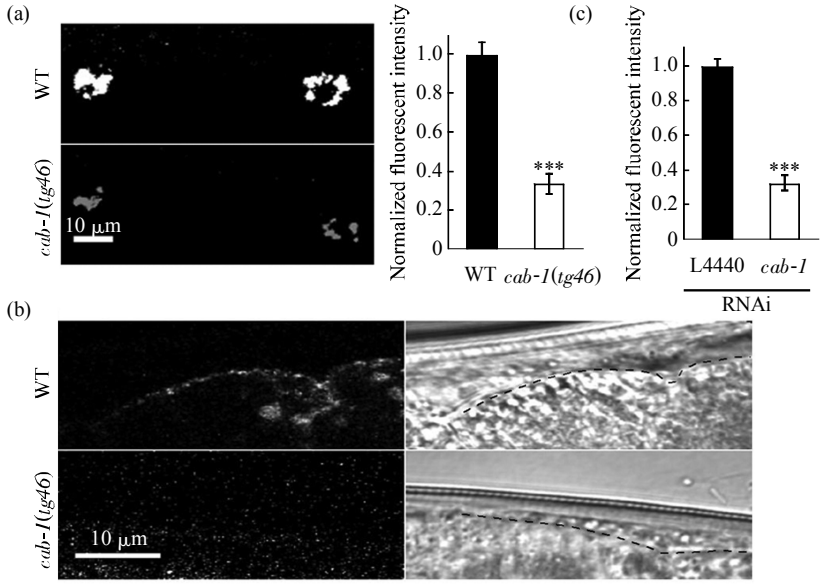

Fig. 3 CAB-1 functions in the intestine to regulate DCV secretion

(a) Representative images of NLP-40-YFP in the coelomocytes of the WT (n=28) and *cab-1*(*tg46*) (n=20) worms (left) and quantification of the fluorescence intensity (right). (b) NLP-40-YFP accumulated at the basolateral region in WT, but the accumulation could be hardly seen in *cab-1*(*tg46*) mutants. Dash line in the DIC image indicates the basolateral membrane. (c) The statistics of the AEX-5-Venus level in worms treated with *cab-1* RNAi showed a similar reduction in the coelomocytes. n=16 for WT and n=17 for *cab-1*(*tg46*) mutants.

2.4 CAB-1 functions in the nervous system to regulate DCV secretion

Previously, Kouichi *et al.*[37] showed that CAB-1 was primarily expressed in the nervous system and that *cab-1* (*tg46*) mutants exhibited phenotypes associated with defective neuronal secretion, such as aldicarb resistance. Therefore, we asked whether CAB-1 also affects neuronal secretion. We first introduced SNB-1-GFP to check the SVs. In the WT worms, SNB-1-GFP puncta were distributed evenly along the dorsal cord, which was similarly observed in the *cab-1* (*tg46*)mutants(Figure S1 in **Supplementary material**).

In addition, the average fluorescence intensity and puncta density in the *cab-1* (*tg46*) mutants were indistinguishable from those in the WT (Figure S1 in **Supplementary material**). These results suggested that the SVs in the *cab-1* (*tg46*) mutants have no significant abnormalities.

Next, we focused on neuronal DCVs. Atrial natriuretic factor (ANF), which has previously been used as a marker for DCV luminal cargoes in both *C. elegans*[15] and *Drosophila*[39], is released in a manner similar to that of endogenous neuropeptides. The *C. elegans* IDA-1 protein is homologous to the mammalian protein phogrin and has been used as a specific DCV-membrane marker [40]. We used GFP-labeled ANF and IDA-1 to examine DCV secretion in the *cab-1* (*tg46*) mutants. As shown in Figure 4, ANF-GFP accumulated in the nerve ring and dorsal cord of the *cab-1* (*tg46*) mutants, and the GFP signal significantly decreased in the coelomocytes (Figure 4a and b), indicating that the secretion of the DCV luminal cargoes is blocked. Consistently, IDA-1-GFP also accumulated in the neuron cell body and axon (Figure 4c and d). Taken together, these results demonstrated that CAB-1 also functions in the nervous system to specifically regulate the trafficking and secretion of DCVs, but not SVs.

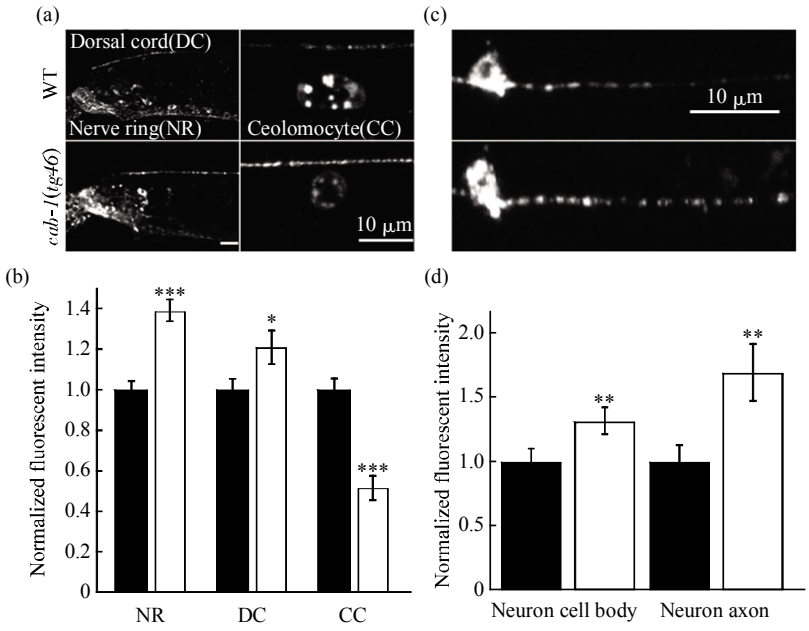

Fig. 4 Neuronal DCV secretion was blocked in *cab-1* (*tg46*) mutants

(a, c) Both DCV luminal cargo ANF-GFP and membrane protein IDA-1-GFP accumulated in the nervous system. Confocal images of different parts are represented. (b, d) The quantification of the fluorescence intensity of the indicated parts. ANF-GFP accumulated in the nerve ring (NR, n=22 for WT and n=23 for *cab-1*(*tg46*) mutants) and dorsal cord (DC, n=20 for WT and n=19 for *cab-1*(*tg46*) mutants), whereas less ANF-GFP was observed in the coelomocytes (n=22 for WT and n=21 for *cab-1*(*tg46*) mutants) (b); IDA-1-GFP significantly increased in the neuron cell body (n=37 for WT and n=38 for *cab-1*(*tg46*) mutants) and axons (n=37 for both WT and *cab-1*(*tg46*) mutants) in the *cab-1*(*tg46*) mutants (d). ■ : WT; □: *cab-1*(*tg46*).

3 Discussion

We performed a whole genome RNAi screen to identify genes that caused DMP defects when knocked down in *C. elegans*. The selected candidates were potentially involved in intestinal DCV formation or secretion. We further showed that the gene *cab-1* is a regulator that functions in DCV exocytosis. We provided evidence that CAB-1 functions in both the intestine and nervous system. In the intestine, mutation of *cab-1* caused the reduced secretion of the DCV cargoes, most likely by regulating the abundance of ready-to-release DCVs at the basolateral membrane area. In the nervous system, CAB-1 specifically regulated the secretion of DCVs but not of SVs as indicated by various fluorescent protein-labeled markers.

The *C. elegans* DMP consists of three sequential

steps: posterior body wall muscle contraction (pBoc), anterior body wall muscle contraction (aBoc) and expulsion (Exp), with the last step executed by two GABAergic neurons, DVB and AVL [41–42]. The activation of these two neurons is triggered by signaling molecules such as neuropeptide NLP-40, which is secreted from the intestine [25]. Abnormalities in signaling molecule secretion or downstream neuron activation would cause defects in Exp. In our screen, we did not cross *rbf-1* (*js232*) with mutants such as *eri-1* or *lin-15B*, which are often used to enhance the sensitivity of the *C. elegans* nervous system to RNAi treatment [43–44]; therefore, our selected candidate genes potentially function in the intestine because the *C. elegans* intestine is very sensitive to RNAi treatment *via* bacterial feeding [38]. The *aex* genes were identified in a forward genetic screen [30], and the intestinal expression of AEX-1, AEX-4 and AEX-5 fully rescued the defecation defect of the respective mutants, suggesting the intestinal functions of these genes [24, 35]. In our screen, *aex-1*, *4* and *5* were successfully identified. In contrast, one *aex* gene, *aex-3*, was occasionally observed with the DMP defect and was thus excluded from the final candidates. Similarly, genes such as *unc-2*, *unc-64* and *kin-1*, which function in the nervous system to regulate DMPs [45], were also included in the PC list (Table S1 in Supplementary material) but were not in the final candidates. These results suggested that our screen is sufficient to discover genes that function in the intestine.

cab-1 was first identified as the C-terminus-binding protein of AEX-3, known as a RAB-3 GEF, in a yeast two-hybrid screen [37], but little was known about its functions. The *cab-1* mutant worms lost almost all the Exp steps (Figure 1a), similar to the *nlp-40* and *aex* mutants [25, 30, 37]. When we examined the secretion of NLP-40 in the *cab-1* mutant, approximately 30% of the WT level was still observed, which did not coincide with the observed greater than 90% DMP defect. A refractory period was proposed to exist that restricts the Exp step from occurring outside of a small window within a few seconds of the pBoc step [24–25]. Thus it is reasonable that the remaining secretion of NLP-40 does not trigger a robust Exp if it is secreted during the refractory period. Similar to NLP-40, AEX-5-Venus secretion was reduced. These evidences supported the notion that CAB-1 regulates the overall secretion of intestinal DCVs.

Because CAB-1 was also reported to be expressed in the nervous system [37], we detected neuronal secretion. The *C. elegans* nervous system primarily produces two types of vesicles, DCVs and SVs, to deliver signaling molecules, and both are crucial for normal behavior and development. As expected, neuronal DCV secretion was blocked in the *cab-1* mutants, but the SVs were not affected. Previously, CAB-1 was proposed to regulate neuronal activities through AEX-3 and was distinct from the well-known RAB-3-AEX-3 pathway, but no specific evidence was provided [37]. Our results indicated that DCVs, instead of SVs, which are regulated by the RAB-3-AEX-3 pathway, is the CAB-1 substrate. AEX-3 has been shown to exert GEF activity toward both *C. elegans* RAB-3 and RAB-27/AEX-6, the latter of which, when mutated, also exhibited similar Exp defect with *cab-1* mutant [46], thus CAB-1 may function through the AEX-3-AEX-6 pathway to regulate the secretion of DCVs. Thus, we identified a new gene that specifically functions in the DCV secretion pathway. Except for DMPs, the *cab-1* mutant also exhibited developmental defects (Figure 2) similar to *unc-64*, which disrupts both development and neuronal secretion when mutated [47]. DCV is considered to be the primary carrier for neuropeptides and hormones, and therefore, this may also explain the developmental defects observed in the *cab-1*(*tg46*) mutants.

Acknowledgements We thank Dr. Derek Sieburth (University of Southern California) for providing the OJ1160 *vjEx555*[*Pttx-3*::*RFP*, *Pnlp-40*::*nlp-40*::*YFP* at 1 mg/L] strain, Dr. Thomas F.J. Martin (University of Wisconsin-Madison) for the *oxIs206*[*Paex-3*::*proANF*::*gfp*] strain, Dr. Joshua M. Kaplan (Harvard Medical School) for the *nuIs152* [*Punc-129*::*snb-1*::*gfp*] strain and Dr. Kennith G. Miller (Oklahoma Medical Research Foundation) for the *ceIs72*[*Punc-129*:*ida-1*::*gfp*] strain. And some strains were provided by the CGC, which is funded by NIH Office of Research Infrastructure Programs (P40 OD010440).

Supplementary material Figure S1 and Table S1, are available at PIBB website(http://www. pibb.ac.cn)

References

[1] Burgoyne R D, Morgan A. Secretory granule exocytosis. Physiological Reviews, 2003, **83**(2): 581−632

[2] Sudhof T C. The synaptic vesicle cycle. Annual Review of

Neuroscience, 2004, **27**: 509−547

[3] Wendler F, Page L, Urbe S, *et al*. Homotypic fusion of immature secretory granules during maturation requires syntaxin 6. Mol Biol Cell, 2001, **12**(6): 1699−1709

[4] Tooze S A, Martens G J, Huttner W B. Secretory granule biogenesis: rafting to the SNARE. Trends Cell Biol, 2001, **11**(3): 116−122

[5] Urbe S, Page L J, Tooze S A. Homotypic fusion of immature secretory granules during maturation in a cell-free assay. J Cell Biol, 1998, **143**(7): 1831−1844

[6] Orci L, Ravazzola M, Amherdt M, *et al*. Conversion of proinsulin to insulin occurs coordinately with acidification of maturing secretory vesicles. J Cell Biol, 1986, **103**(6 Pt 1): 2273− 2281

[7] Schoonderwoert V T, Holthuis J C, Tanaka S, *et al*. Inhibition of the vacuolar H^+-ATPase perturbs the transport, sorting, processing and release of regulated secretory proteins. Euro J Biochem/FEBS, 2000, **267**(17): 5646−5654

[8] Taupenot L, Harper K L, O'Connor D T. Role of H^+-ATPase-mediated acidification in sorting and release of the regulated secretory protein chromogranin A: evidence for a vesiculogenic function. J Biol Chem, 2005, **280**(5): 3885−3897

[9] Hinners I, Wendler F, Fei H, *et al*. AP-1 recruitment to VAMP4 is modulated by phosphorylation-dependent binding of PACS-1. EMBO Reports, 2003, **4**(12): 1182−1189

[10] Bonnemaison M L, Eipper B A, Mains R E. Role of adaptor proteins in secretory granule biogenesis and maturation. Frontiers in Endocrinology, 2013, **4**: 101

[11] Zahn T R, Angleson J K, Macmorris M A, *et al*. Dense core vesicle dynamics in *Caenorhabditis elegans* neurons and the role of kinesin UNC-104. Traffic, 2004, **5**(7): 544−559

[12] Jacob T C, Kaplan J M. The EGL-21 carboxypeptidase E facilitates acetylcholine release at *Caenorhabditis elegans* neuromuscular junctions. J Neurosci, 2003, **23**(6): 2122−2130

[13] Takamori S, Holt M, Stenius K, *et al*. Molecular anatomy of a trafficking organelle. Cell, 2006, **127**(4): 831−846

[14] Lin X G, Ming M, Chen M R, *et al*. UNC-31/CAPS docks and primes dense core vesicles in *C. elegans* neurons. Biochem Biophys Res Commun, 2010, **397**(3): 526−531

[15] Speese S, Petrie M, Schuske K, *et al*. UNC-31 (CAPS) is required for dense-core vesicle but not synaptic vesicle exocytosis in *Caenorhabditis elegans*. J Neurosci, 2007, **27**(23): 6150−6162

[16] Sieburth D, Madison J M, Kaplan J M. PKC-1 regulates secretion of neuropeptides. Nat Neurosci, 2007, **10**(1): 49−57

[17] Fire A, Xu S, Montgomery M K, *et al*. Potent and specific genetic interference by double-stranded RNA in *Caenorhabditis elegans*. Nature, 1998, **391**(6669): 806−811

[18] Tabara H, Grishok A, Mello C C. RNAi in *C. elegans*: soaking in the genome sequence. Science, 1998, **282**(5388): 430− 431

[19] Timmons L, Court D L, Fire A. Ingestion of bacterially expressed dsRNAs can produce specific and potent genetic interference in *Caenorhabditis elegans*. Gene, 2001, **263**(1−2): 103− 112

[20] Kamath R S, Fraser A G, Dong Y, *et al*. Systematic functional analysis of the *Caenorhabditis elegans* genome using RNAi. Nature, 2003, **421**(6920): 231−237

[21] Rual J F, Ceron J, Koreth J, *et al*. Toward improving *Caenorhabditis elegans* phenome mapping with an ORFeome-based RNAi library. Genome Research, 2004, **14**(10B): 2162−2168

[22] Lynch A M, Grana T, Cox-Paulson E, *et al*. A genome-wide functional screen shows MAGI-1 is an L1CAM-dependent stabilizer of apical junctions in *C. elegans*. Curr Biol, 2012, **22**(20): 1891−1899

[23] Morton D G, Hoose W A, Kemphues K J. A genome-wide RNAi screen for enhancers of par mutants reveals new contributors to early embryonic polarity in *Caenorhabditis elegans*. Genetics, 2012, **192**(3): 929−942

[24] Mahoney T R, Luo S, Round E K, *et al*. Intestinal signaling to GABAergic neurons regulates a rhythmic behavior in *Caenorhabditis elegans*. Proc Natl Acad Sci USA, 2008, **105**(42): 16350−16355

[25] Wang H, Girskis K, Janssen T, *et al*. Neuropeptide secreted from a pacemaker activates neurons to control a rhythmic behavior. Curr Biol, 2013, **23**(9): 746−754

[26] Brenner S. The genetics of *Caenorhabditis elegans*. Genetics, 1974, **77**(1): 71−94

[27] Kamath R S, Martinez-Campos M, Zipperlen P, *et al*. Effectiveness of specific RNA-mediated interference through ingested double-stranded RNA in *Caenorhabditis elegans*. Genome Biology, 2001, **2**(1): RESEARCH0002

[28] Evans T C. Transformation and microinjection. WormBook: the online review of *C. elegans* biology, 2006,

[29] Feng W, Liang T, Yu J, *et al*. RAB-27 and its effector RBF-1 regulate the tethering and docking steps of DCV exocytosis in *C. elegans*. Science China Life Sciences, 2012, **55**(3): 228−235

[30] Thomas J H. Genetic analysis of defecation in *Caenorhabditis elegans*. Genetics, 1990, **124**(4): 855−872

[31] Yu Y, Wang L, Jiu Y, *et al*. HID-1 is a novel player in the regulation of neuropeptide sorting. Biochem J, 2011, **434**(3): 383−390

[32] Mesa R, Luo S, Hoover C M, *et al*. HID-1, a new component of the peptidergic signaling pathway. Genetics, 2011, **187**(2): 467− 483

[33] Sumakovic M, Hegermann J, Luo L, *et al*. UNC-108/ RAB-2 and its effector RIC-19 are involved in dense core vesicle maturation in *Caenorhabditis elegans*. J Cell Biol, 2009, **186**(6): 897−914

[34] Edwards S L, Charlie N K, Richmond J E, *et al*. Impaired dense core vesicle maturation in *Caenorhabditis elegans* mutants lacking Rab2. J Cell Biol, 2009, **186**(6): 881−895

[35] Doi M, Iwasaki K. Regulation of retrograde signaling at neuromuscular junctions by the novel C2 domain protein AEX-1. Neuron, 2002, **33**(2): 249−259

[36] Husson S J, Janssen T, Baggerman G, *et al*. Impaired processing of FLP and NLP peptides in carboxypeptidase E (EGL-21)-deficient *Caenorhabditis elegans* as analyzed by mass spectrometry. J Neurochem, 2007, **102**(1): 246−260

[37] Iwasaki K, Toyonaga R. The Rab3 GDP/GTP exchange factor homolog AEX-3 has a dual function in synaptic transmission.

EMBO J, 2000, **19**(17): 4806−4816

[38] Espelt M V, Estevez A Y, Yin X, *et al*. Oscillatory Ca^{2+} signaling in the isolated *Caenorhabditis elegans* intestine: role of the inositol-1, 4,5-trisphosphate receptor and phospholipases C beta and gamma. The Journal of General Physiology, 2005, **126**(4): 379−392

[39] Husain Q M, Ewer J. Use of targetable gfp-tagged neuropeptide for visualizing neuropeptide release following execution of a behavior. J Neurobiol, 2004, **59**(2): 181−191

[40] Zahn T R, Macmorris M A, Dong W, *et al*. IDA-1, a *Caenorhabditis elegans* homolog of the diabetic autoantigens IA-2 and phogrin, is expressed in peptidergic neurons in the worm. J Comp Neurol, 2001, **429**(1): 127−143

[41] Liu D W, Thomas J H. Regulation of a periodic motor program in *C. elegans*. J Neurosci, 1994, **14**(4): 1953−1962

[42] Mcintire S L, Jorgensen E, Kaplan J, *et al*. The GABAergic nervous system of *Caenorhabditis elegans*. Nature, 1993, **364** (6435): 337−341

[43] Kennedy S, Wang D, Ruvkun G. A conserved siRNA-degrading RNase negatively regulates RNA interference in *C. elegans*. Nature, 2004, **427**(6975): 645−649

[44] Sieburth D, Ch'ng Q, Dybbs M, *et al*. Systematic analysis of genes required for synapse structure and function. Nature, 2005, **436**(7050): 510−517

[45] Wang H, Sieburth D. PKA controls calcium influx into motor neurons during a rhythmic behavior. PLoS Genet, 2013, **9** (9): e1003831

[46] Mahoney T R, Liu Q, Itoh T, *et al*. Regulation of synaptic transmission by RAB-3 and RAB-27 in *Caenorhabditis elegans*. Mol Biol Cell, 2006, **17**(6): 2617−25.

[47] Ogawa H, Harada S, Sassa T, *et al*. Functional properties of the unc-64 gene encoding a *Caenorhabditis elegans* syntaxin. J Biol Chem, 1998, **273**(4): 2192−2198

线虫全基因组 RNAi 筛选确定 CAB-1 为特异性调节致密核心囊泡分泌的因子 *

夏志平[1, 3)**]　陈　艳[1, 3)**]　盛　毅[1, 2)]　易雅岚[1, 3)]　宋婀莉[1)***]　徐　涛[1, 2)***]

([1)] 中国科学院生物物理研究所，生物大分子国家重点实验室，北京 100101；

[2)] 华中科技大学生命科学与技术学院，武汉 430074；[3)] 中国科学院大学，北京 100049)

摘要　内分泌细胞和神经细胞通过释放激素和神经肽类物质来响应外界刺激，而这些物质的分泌，都是通过致密核心囊泡(dense core vesicle，DCV)来实现的．但是，现阶段关于 DCV 的生成、转运、释放的机制很大程度上是不清楚的．在本研究中，我们将线虫的排便行为和肠道分泌联系起来，并以此表型进行全基因组 RNAi 筛选，寻找调节 DCV 的新基因．我们成功筛选到了一些在肠道调节 DCV 生成或释放的基因．其中，CAB-1 被确认为特异性调节 DCV 分泌的重要因子．在肠道中，*cab-1* 突变会降低肠道 DCV 内容物的分泌，而在神经系统中，CAB-1 的缺失也会导致 DCV 的标识物堆积在突触前，而突触囊泡(synaptic vesicle，SV)不受影响．

关键词　CAB-1，线虫排便行为，致密核心囊泡，分泌，全基因组 RNAi 筛选

学科分类号　Q422，Q73　　**DOI**: 10.3724/SP.J.1206.2014.00047

* 国家重点基础研究发展计划(973)(2010CB833701), 国家自然科学基金 (31130065, 31270884, 31300701) 和北京市自然科学基金(5122026)资助项目.

** 共同第一作者.

*** 通讯联系人．Tel: 010-64888469

徐　涛．E-mail: xutao@ibp.ac.cn

宋婀莉．E-mail: songali@moon.ibp.ac.cn

收稿日期：2014-02-21，接受日期：2014-04-16

Supplementary material

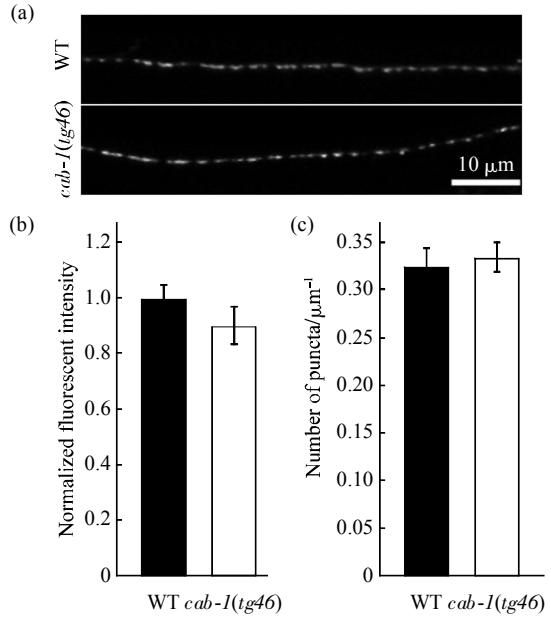

Fig. S1 The synaptic vesicles were not affected in the *cab-1*(*tg46*) mutants

(a) Representative confocal images of SNB-1-GFP in the WT and *cab-1* (*tg46*) worms. (b) The quantification of the average fluorescence intensity of SNB-1-GFP showed no difference between WT (n=29) and *cab-1* (*tg46*) (n=25). (c) The puncta density of SNB-1-GFP was also indistinguishable. 9 axons for both WT and *cab-1* (*tg46*) mutants were analyzed.

Table S1 Potential candidates (PCs) were listed

Locus	Gene	Description[a]
unc-108	F53F10.4	Small GTPase RAB-2
clec-89	C09D1.2	C-type lectin
	C18E3.3	U[b]
	C41D11.4	U
	T04D1.2	U
	F54D7.2	Ethanolaminephosphotransferase
ckr-1	T23B3.4	Cholecystokinin receptor
	C37A2.7	Ribosomal protein
unc-15	F07A5.7	Paramyosin
aex-1	D2030.10	Munc13 homolog
hsr-9	T05F1.6	Protein containing a BRCT (BRCA 1 C terminus) domain
	Y106G6D.3	Splicing regulatory glutamine/lysine-rich protein 1 homolog
ska-1	Y106G6H.15	Spindle and Kinetochore-Associated protein
mafr-1	C43H8.2	MAF Polymerase Ⅲ Regulator homolog
fkb-7	B0511.1	Peptidylprolyl cis/trans isomerase
	Y52B11C.1	N-acetylglucosaminyl-phosphatidylinositol de-N-acetylase
	F36D1.5	U
acox-1	F08A8.1	Peroxisomal acyl-coenzyme A oxidase
taf-1	W04A8.7	TATA-binding protein associated factor
best-11	C49A1.3	Bestrophin
rps-20	Y105E8A.16	Small ribosomal subunit
aex-5	F32A7.6	Prohormone convertase
cogc-3	Y71F9AM.4	Conserved oligomeric Golgi complex subunit
	W04H10.1	U
	C08G5.3	Vitelline membrane outer layer protein
lin-42	F47F6.1	Period circadian protein homolog
fgt-1	H17B01.1	Facilitated glucose transporter
btb-8	F45C12.6	U
fbxa-184	F45C12.8	F-box A protein
him-14	ZK1127.11	MutS protein homolog
gei-4	W07B3.2	GEX Interacting protein
snt-2	F42G9.7	Synaptotagmin
	T15B12.2	Casein kinase
nmt-1	T17E9.2	N-Myristoyl Transferase homolog
	F23F12.7	Merged into F23F12.8
ykt-6	B0361.10	Synaptobrevin
lin-39	C07H6.7	Homeobox protein
snap-29	K02D10.5	Synaptosomal-associated protein
prx-19	F54F2.8	Peroxisomal biogenesis factor
rheb-1	F54C8.5	GTP-binding protein Rheb
	ZK1128.3	U
fbxb-24	Y56A3A.15	F-box B protein
trap-4	Y56A3A.21	Translocon-associated protein subunit
arx-3	Y79H2A.6	Actin-related protein 2/3 complex subunit
epg-3	Y37D8A.22	Ectopic P Granules
mlc-5	T12D8.6	MLC3 of Myosin light chain
	Y22D7AR.7	U
col-101	K02D7.3	Cuticle collagen
	C34H4.2	U
cyc-2.1	E04A4.7	Cytochrome c protein
rpl-20	E04A4.8	Large ribosomal subunit
tre-2	T05A12.2	Putative trehalase
cogc-2	C06G3.10	Conserved oligomeric Golgi complex subunit
	F20D12.7	U

Continued

Locus	Gene	Description[a]
arf-3	F57H12.1	ADP-ribosylation factor
pme-4	H23L24.5	Poly(ADP-ribose) glycohydrolase
ndc-80	W01B6.9	Kinetochore protein
let-70	M7.1	Class Ⅰ E2 ubiquitin conjugating enzyme
	ZK809.5	U
sec-24.2	ZC518.2	Yeast SEC homolog
	F08G5.6	U
	C27H2.3	Merged into C27H2.2
	Y37A1B.7	U
	Y51H4A.16	U
egl-8	B0348.4	Phospholipase C
	T20D4.10	U
klc-2	C18C4.10	Kinesin light chain
atp-4	T05H4.12	ATP synthase subunit
syx-18	T10H9.3	Syntaxin-18
smk-1	F41E6.4	Serine/threonine-protein phosphatase regulatory subunit
gcy-33	F57F5.2	Soluble guanylate cyclase beta subunit
	K01D12.5	U
srh-25	C54D10.6	Serpentine Receptor
	W04D2.6	RNA-binding protein
	R11D1.2	U
	ZC443.1	Aldose reductase
eif-3.K	T16G1.11	Translation initiation factor subunit
lap-2	W07G4.4	Zinc metalloprotease leucine aminopeptidase
clec-225	B0365.5	C-type lectin
sun-1	F57B1.2	SUN-domain protein
glb-22	R11H6.3	Globin
clec-29	T25E12.9	C-type lectin
srh-216	T20B3.5	Serpentine Receptor
	C14B4.2	U
acs-12	F25C8.4	Fatty Acid CoA Synthetase
	Y61A9LA.5	U
aex-3	C02H7.3	GEF for the RAB-3 GTPase
hid-1	K02E10.2	U
	F54G2.2	Kinectin
unc-2	T02C5.5	Calcium channel alpha subunit
dpy-23	R160.1	AP-2 complex subunit mu
inx-5	R09F10.4	Innexin family
elt-2	C33D3.1	GATA-type transcription factor
slcf-1	F59F5.1	Solute Carrier Family
bet-2	F57C7.1	Bromodomain-containing protein
abl-1	M79.1	Tyrosine-protein kinase
	C05A9.2	U
ttyh-1	F42E11.2	Protein tweety homolog
	T04F8.2	Transmembrane protein
	Y62H9A.7	U
cab-1	C23H4.1	AEX-3 binding protein
pab-2	F18H3.3	Polyadenylate-binding protein
ekl-5	Y26E6A.1	U
ntr-2	F14F4.1	Nematocin Receptor
	F36D4.2	Trafficking protein particle complex subunit
unc-64	F56A8.7	Syntaxin-1
	F56C9.12	U
	F56A8.3	Leucine-rich repeat-containing protein
kin-1	ZK909.2	cAMP-dependent protein kinase catalytic subunit
pfs-2	R06A4.9	Polyadenylation Factor Subunit homolog
arx-4	Y6D11A.2	Actin-related protein 2/3 complex subunit
nlp-40	Y74C9A.2	Neuropeptide
cogc-4	Y51H7C.6	Conserved oligomeric Golgi complex subunit
twk-39	C24H11.8	TWiK family of potassium channels
	Y39A3CL.3	U
ast-1	T08H4.3	ETS-box transcription factors
egl-21	F01D4.4	Carboxypeptidase
aex-4	T14G12.2	SNAP-25

[a]Descriptions summarized from Wormbase (http://www.wormbase.org/); [b]Function unknown or uncharacterized.